A novel protein kinase D phosphorylation site in the tumor suppressor Rab interactor 1 is critical for coordination of cell migration

Susanne Ziegler[a], Tim Eiseler[a], Rolf-Peter Scholz[a], Alexander Beck[b], Gisela Link[a], and Angelika Hausser[a]
[a]Institute of Cell Biology and Immunology, University of Stuttgart, 70569 Stuttgart, Germany; [b]Panatecs GmbH, 72070 Tübingen, Germany

ABSTRACT The multifunctional signal adapter protein Ras and Rab interactor 1 (RIN1) is a Ras effector protein involved in the regulation of epithelial cell processes such as cell migration and endocytosis. RIN1 signals via two downstream pathways, namely the activation of Rab5 and Abl family kinases. Protein kinase D (PKD) phosphorylates RIN1 at serine 351 in vitro, thereby regulating interaction with 14–3-3 proteins. Here, we report the identification of serine 292 in RIN1 as an in vivo PKD phosphorylation site. PKD-mediated phosphorylation at this site was confirmed with a phospho-specific antibody and by mass spectrometry. We demonstrate that phosphorylation at serine 292 controls RIN1-mediated inhibition of cell migration by modulating the activation of Abl kinases. We further provide evidence that RIN1 in vivo phosphorylation at serine 351 occurs independently of PKD. Collectively, our data identify a novel PKD signaling pathway through RIN1 and Abl kinases that is involved in the regulation of actin remodeling and cell migration.

INTRODUCTION

The Ras and Rab interactor 1 (RIN1) was originally identified as a Ras effector that directly interacts with active Ras (Han and Colicelli, 1995; Wang and Colicelli, 2001). RIN1 is highly expressed in neuronal tissue but is also present in some epithelial cells (e.g., mammary epithelial cells [MEC]) as well as HeLa cells (Bliss et al., 2005). The RIN1 protein is structured into four functional domains (detailed in Bliss et al., 2005). The amino terminal half of RIN1 contains a SRC homology 2 (SH2) domain as well as proline-rich domains. The car-

boxyl-terminal section of RIN1 contains a Ras association and a guanine nucleotide exchange factor (GEF) domain of the subclass most related to the vacuolar protein sorting 9 protein. In addition to active Ras proteins, several interaction partners have been identified, including Rab5 (Tall et al., 2001), Abl tyrosine kinases (Afar et al., 1997; Hu et al., 2005), signal-transducing adapter molecule (STAM) (Kong et al., 2007), epidermal growth factor receptor (EGFR) (Barbieri et al., 2003), and 14–3-3 proteins (Wang et al., 2002). Two downstream pathways for RIN1 have been described so far: First, RIN1 has GEF activity for Rab5, thereby directly activating Rab5-mediated endocytosis of several receptor tyrosine kinases such as EGFR (Tall et al., 2001; Barbieri et al., 2003; Barbieri et al., 2004), likely via its interaction with STAM (Kong et al., 2007). The Rab5 GEF activity of RIN1 also seems to be important in vivo. RIN1 expression is highest in the postnatal brain (Han et al., 1997). Conversely, RIN1$^{-/-}$ mice showed increased long-term potentiation (LTP) in the amygdala and displayed enhanced fear conditioning, suggesting a role for RIN1 in neuronal plasticity (Dhaka et al., 2003). In amygdala neurons RIN1 directly interacts with ephrin type-A receptor 4 (EphA4) and mediates its endocytosis in a Rab5-dependent manner, thereby antagonizing EphA4 signaling (Deininger et al., 2008). This signaling pathway may contribute to the regulation of LTP.

The second RIN1-regulated pathway is the direct interaction and activation of Bcr-Abl and Abl/Arg tyrosine kinases (Afar et al., 1997; Hu et al., 2005). RIN1 binds to the SH3 and SH2 domains of c-Abl and Arg, thereby stimulating kinase activity. The induction of kinase

activity is independent of other regulatory mechanisms, such as Src-mediated phosphorylation (Cao et al., 2008). It is believed that RIN1 binding to Abl kinases induces a conformational change that leads to a relief of autoinhibition (Cao et al., 2008). Subsequently, RIN1 becomes tyrosine phosphorylated by Abl kinases, a process further stabilizing the interaction of the two proteins. RIN1-mediated activation of Abl kinases is followed by increased phosphorylation of the Abl kinase substrate CrkL and finally by the inhibition of cell migration. Importantly, the direct activation of Abl family kinases through RIN1 is enhanced by activated Ras (Hu et al., 2005). These findings are further supported by studies with RIN1$^{-/-}$ MECs, which demonstrate an increased migration potential compared to wild-type (WT) MECs. Accordingly, knockdown of RIN1 in human epithelial cell lines leads to the same phenotype. Interestingly, RIN1 is silenced in breast tumor cell lines compared to cultured MECs. Silencing likely occurs via DNA methylation within the RIN1 promoter snail is not an abbreviation and/or overexpression of the transcription repressor SNAII (Milstein et al., 2007). A recent study presented evidence that transforming growth factor-β, a key regulator of epithelial-mesenchymal transition, and receptor tyrosine kinases cooperate to silence RIN1 through expression of SNAII. The depletion of RIN1 enhances growth factor–directed cell migration of breast tumor cells (Hu et al., 2008). Therefore, RIN1 has been characterized as a breast tumor suppressor protein acting as a negative regulator of tumor cell invasive growth (Milstein et al., 2007). Taken together, RIN1 is involved in signaling pathways promoting endocytosis and actin cytoskeleton remodeling.

In the past, Wang and coworkers identified serine 351 within RIN1 as an in vitro phosphorylation site for protein kinase D (PKD). Phosphorylation of this serine residue mediates binding of RIN1 to 14–3-3 proteins and in part regulates interaction of RIN1 with active Ras (Wang et al., 2002). PKD is a family of serine/threonine kinases, the function of which has been studied best at the Golgi complex where it is known to regulate vesicular traffic to the plasma membrane (reviewed in Wang, 2006). More recent studies by us and other laboratories suggest that PKD has additional functions associated with the regulation of cell shape, migration, and invasion. Only a few substrates, however, such as cortactin, E-Cadherin, and slingshot 1L (SSH1L) have been identified so far (Jaggi et al., 2005; Eiseler et al., 2009, 2010; Peterburs et al., 2009). By using a phosphospecific antibody, we now demonstrate that RIN1 is phosphorylated on serine 351 in vivo, but independently of PKD. Instead, we report the identification of a novel PKD phosphorylation site, serine 292, in RIN1. We demonstrate that phosphorylation at this site occurs in vitro and in vivo. We further provide evidence that serine 292 phosphorylation regulates RIN1-dependent activation of Abl kinases and, as a consequence, controls directed migration of epithelial cells.

RESULTS

A novel phosphorylation site in RIN1 is detected by the PKD pMOTIF antibody

Both PKD and its substrate RIN1 act as negative regulators of directional cell migration (Hu et al., 2005; Eiseler et al., 2007). Whether both proteins are part of a common pathway that inhibits cell migration has not been addressed, however. When ectopically expressed in HEK293T cells, Flag-tagged WT RIN1 reacts with the phospho-specific PKD pMOTIF antibody (Figure 1A), which specifically detects phosphorylated PKD consensus motifs (Doppler et al., 2005). Interestingly, mutation of the putative PKD phosphorylation site at serine 351 did not fully abrogate the detection of the protein with the pMOTIF antibody (Figure 1A), suggesting the presence of ad-

ditional phosphorylated serine residues within RIN1. To identify these pMOTIF recognition sites in RIN1, we searched for potential PKD consensus motifs characterized by a leucine, isoleucine, or valine residue in the -5 and arginine in the -3 position relative to a serine or threonine. Besides serine 351, two additional serines at positions 291 and 292 match the PKD consensus motif and are conserved across species (Figure 1B). These residues were exchanged for alanines by site-directed mutagenesis, and the mutants were expressed in HEK293T cells and further tested for recognition by the pMOTIF antibody. Mutation of serine 292 to alanine abrogated detection of RIN1 with the pMOTIF antibody, whereas the S291A mutation did not affect the pMOTIF signal (Figure 1C). This finding suggested that serine 292 is a novel PKD phosphorylation site specifically recognized by the PKD substrate antibody. To confirm that serine 292 is phosphorylated in vivo we performed mass spectrometry. To this end, Flag-tagged RIN1 WT was purified from HEK293T cell lysates using Flag-M2-agarose. To increase the amount of phosphorylated RIN1 molecules we coexpressed a constitutively active PKD1 protein. Using nano-liquid chromatography electrospray ionization tandem mass spectrometry (nanoLC/ESI-MS/MS; Figure 1D, top) the tryptically digested Flag-RIN1 fusion protein could be unambiguously identified based on the uninterpreted MS/MS spectra (MASCOT Mowse Score 2922). For target MS/MS analyses of the monophosphorylated tryptic peptide RESSVGYR (corresponding to residues 289–296 in full-length human RIN1), the doubly charged precursor ion at m/z 517.27 (Figure 1D, middle, left panel) was chosen as a preferred mass. In the tandem mass spectrum of the m/z 517.27 precursor ion, an intense peak at m/z 468.25 (49.0 Da mass difference, 98/2 Da) could be observed showing the neutral loss of phosphoric acid from the precursor ion (Figure 1D, middle, right panel). Based on the MS/MS data the phosphorylation site could be determined as serine 292 by the presence of the y- and b-ion series (Figure 1D, bottom). Furthermore, the four previously described phosphorylation sites (tyrosine 36, serines 333 and 337, serine 351) (Wang et al., 2002; Zhang et al., 2005; Beausoleil et al., 2006) were also detected during the analysis (Supplemental Figure 1).

To further investigate the phosphorylation of RIN1 at serines 292 and 351 in intact cells, we raised phospho-specific antibodies against the peptide epitope surrounding these residues in RIN1. WT Flag-RIN1 was detected with the pS292 and pS351-specific antibodies, whereas the respective serine-to-alanine exchange mutants, Flag-RIN1 S292A and S351A, were not detected (Figure 1E). Furthermore, a RIN1 variant mutated at both sites was not detectable with either antibody. Together, our results demonstrate that serine 292 is a novel in vivo phosphorylation site specifically recognized by the PKD substrate antibody.

Serine 292 but not serine 351 is a target site for PKD in vivo
Mass spectrometry and Western blot analysis identified serine 292 as a novel in vivo phosphorylation site. To confirm that PKD was indeed capable of directly phosphorylating serine 292 in RIN1, we performed in vitro kinase assays with purified PKD1 and Flag-tagged RIN1 WT, RIN1-S351A, RIN1-S292A, and a RIN1 protein with both serines exchanged for alanines (RIN1-S292/351A). When the RIN1 WT protein was incubated with PKD1 in the presence of [γ-^{32}P]-ATP, incorporation of radioactivity was detected (Figure 2A). Phosphorylation was substantially impaired only in the case of the RIN1-S292/351A protein, indicating that both sites, serines 292 and 351, are phosphorylated by PKD in vitro. To investigate whether in vivo phosphorylation of serines 292 and 351 was dependent on PKD kinase activity, we used Flp-In T-REx-293 cells that stably express the Tet repressor and contain a single genomic Flp recombination
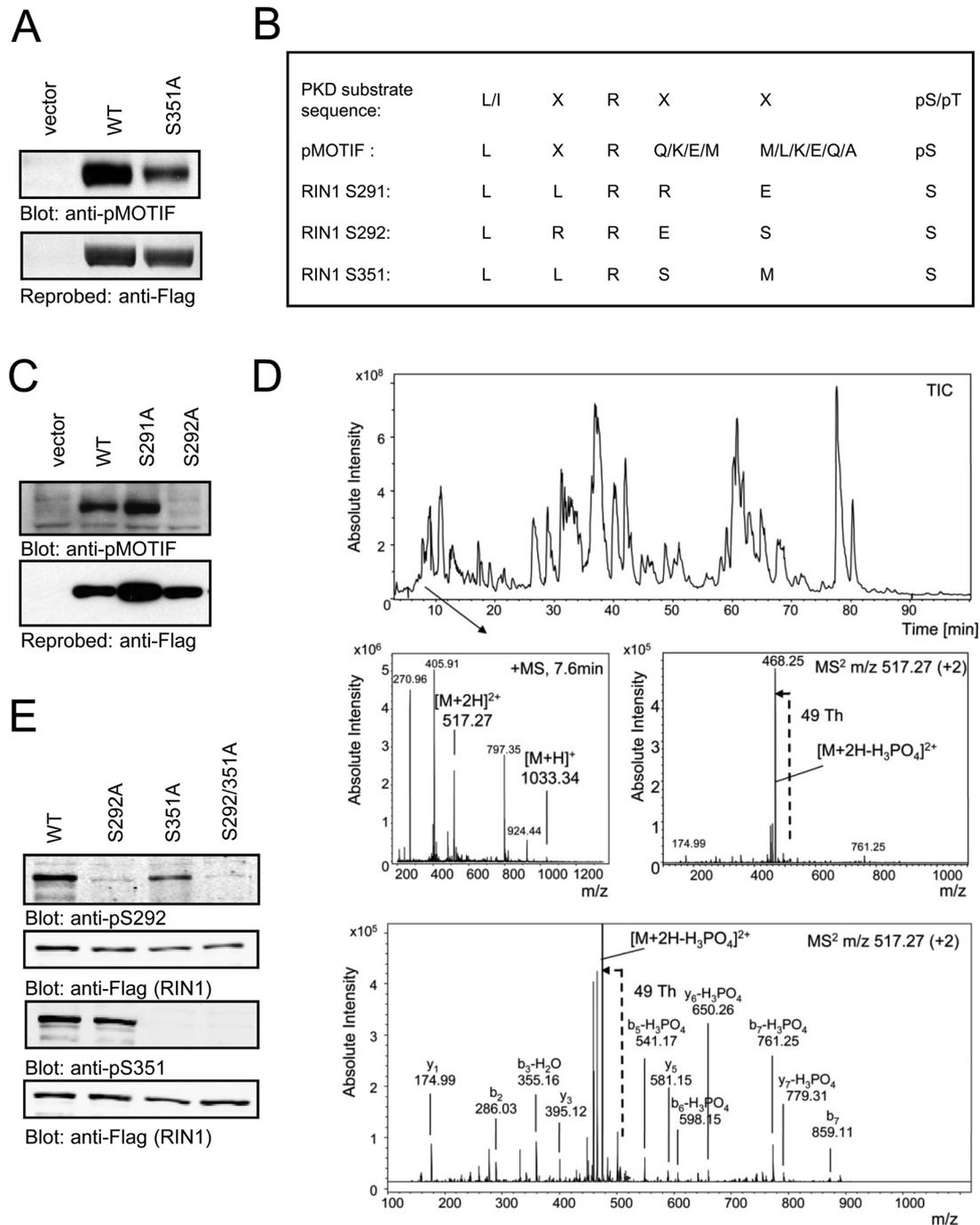
FIGURE 1: A novel phosphorylation site in RIN1 is detected by the PKD pMOTIF antibody. (A) HEK293T cells were transfected with expression plasmids encoding Flag-tagged RIN1 WT and RIN1-S351A. Cells were lysed 24 h post-transfection, and proteins were subjected to SDS–PAGE, followed by immunoblotting with PKD substrate antibody (pMOTIF; top panel) and, after stripping, with anti-Flag antibody (bottom panel). (B) Alignment of the peptide sequences used to raise the PKD substrate antibody and the four potential PKD motifs in RIN1. (C) HEK293T cells were transfected with expression plasmids encoding Flag-tagged RIN1 WT, RIN1-S291A, and RIN1-S292A. The cells were lysed, and RIN1 proteins were analyzed by Western blotting as described in A. (D) NanoLC/ES-MS/MS analysis of the tryptically digested Flag-RIN1 fusion protein. Top, Total ion chromatogram (TIC); middle, ES mass spectrum acquired during the elution of the phosphorylated peptide RESSVGYR (amino acid 289–296; Swiss-Prot entry Q13671) (left panel). Product ion spectrum acquired from the doubly charged precursor ion at m/z 517.27 (right panel). As a result of gas phase elimination of H_3PO_4 from the precursor ion (loss of 98/2 Da), an intense $[M+2H-H_3PO_4]^{2+}$ neutral loss fragment ion at m/z 468.25 was formed (Th: Thompson). Bottom, Interpretation of the tandem mass spectrum shown in the middle panel. Based on the MS/MS data, the position of the phosphorylation site could be determined at serine 292. (E) HEK293T cells were transfected with expression plasmids encoding Flag-tagged RIN1 WT, S292A, S351A, and S292/351A. Cells were lysed 24 h posttransfection, and proteins were subjected to SDS–PAGE, followed by immunoblotting with the pS292- and pS351-specific antibodies, respectively, and with anti-Flag antibody.
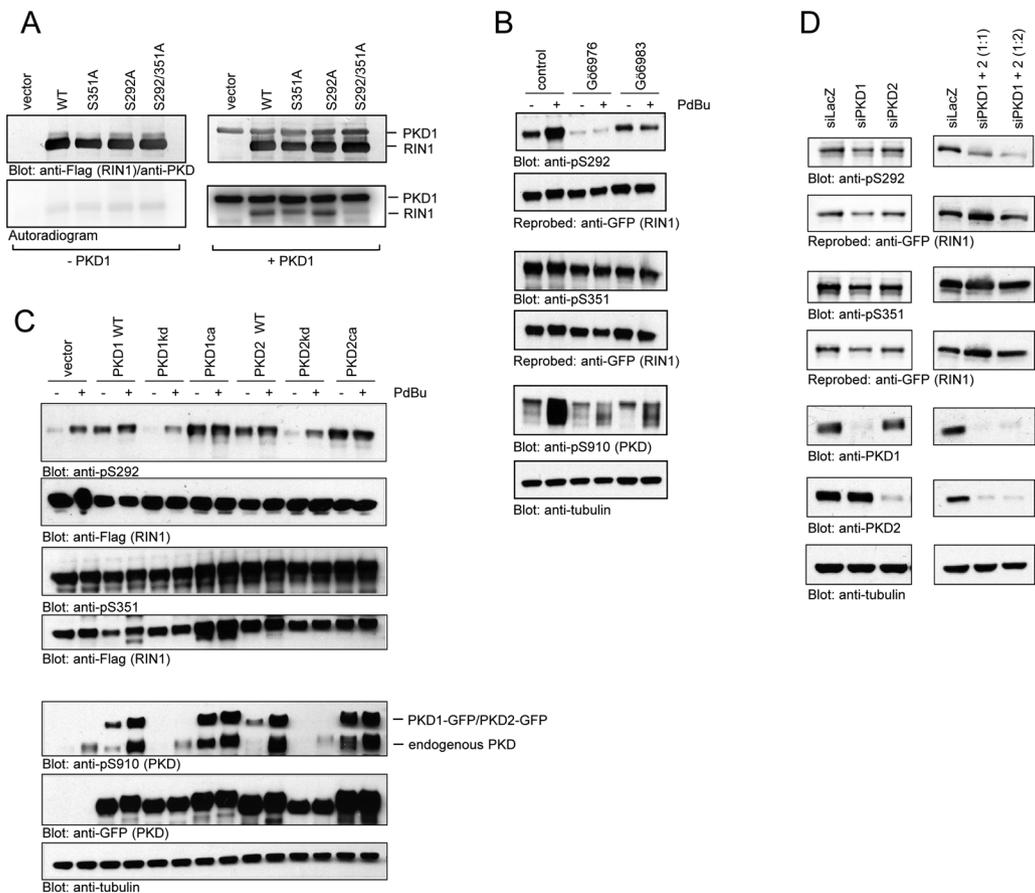
FIGURE 2: PKD1 and PKD2 phosphorylate RIN1 on serine 292. (A) HEK293T cells were transfected with expression plasmids encoding Flag-tagged RIN1 WT, S351A, S292A, and S292/351A fusion proteins. RIN1 variants were immunoprecipitated with anti-Flag-antibody and incubated in kinase buffer containing [^{32}P]-γ-ATP in the absence (–) and presence (+) of purified PKD1 for 10 min. Proteins were separated by SDS–PAGE and transferred to membrane. Incorporation of radioactive phosphate was analyzed using a PhosphoImager (bottom), followed by immunoblotting with Flag-specific and PKD-specific antibodies to verify equal loading of the RIN1 and PKD1 proteins (top), respectively. (B) Flp-In T-Rex-293-GFP-RIN1 WT cells were treated with doxycycline for 24 h to induce RIN1 expression followed by treatment with Gö6976 or Gö6983 at 10 μM prior to stimulation with PDBu (1 μM) for 15 min. Phosphorylation of RIN1 was analyzed in whole cell lysates as described in Figure 1E. PKD autophosphorylation was verified by immunoblotting of whole cell lysates with specific antibodies (middle panel), and equal loading was controlled with a tubulin-specific antibody (bottom panel). (C) HEK293T cells were transfected with Flag-RIN1 together with empty vector, PKD1-GFP WT, PKD1ca-GFP, PKD1kd-GFP, PKD2-GFP WT, PKD2ca-GFP, and PKD2kd-GFP expression plasmids. Cells were left untreated or stimulated with PDBu. Phosphorylation of RIN1 (pS292 and pS351) and PKD proteins (pS910) was analyzed by Western blotting as described in Figures 1E and 2B. Expression of RIN1 and PKD1 and PKD2 proteins was verified by immunoblotting with Flag- and GFP-specific antibody, respectively. Shown is a representative Western blot. (D) Flp-In T-REx-293-GFP-RIN1 WT cells were transfected with lacZ-, PKD1-, and PKD2-specific siRNAs as indicated. RIN1 expression was induced 48 h later and analyzed by immunoblotting as described in Figure 1E (top panels). Silencing of PKD1 and PKD2 isoforms was verified by immunoblotting of whole cell lysates with specific antibodies (middle panels), and equal loading was controlled with a tubulin-specific antibody (bottom panel).

target (FRT) site to generate cells inducibly expressing RIN1 by Flp recombinase–mediated integration of the green fluorescent protein (GFP)-tagged RIN1 cDNA under the control of a tetracycline regulatable promoter. In these cells, GFP-RIN1 expression was tightly controlled, with no expression observed in the absence of doxycycline (see Figure 4A later in the paper). We treated these stable Flp-In-GFP-RIN1 WT cells with the phorbol 12,13-dibutyrate (PDBu), which is known to stimulate PKD in a protein kinase C (PKC)-dependent manner (Wang, 2006). Treatment with PDBu increased PKD kinase activity, based on enhanced PKD autophosphorylation on serine 910 (Figure 2B). Moreover, phosphorylation of RIN1 at serine 292 was strongly increased under these conditions. Treatment of control or PDBu-treated cells with the PKD inhibitor Gö6976 or with the PKC inhibitor Gö6983 resulted in the inhibition of PKD kinase

activity and subsequently in a decrease of serine 292 phosphorylation as judged from detection with the pS292 antibody (Figure 2B). Of note, treatment of cells with Gö6983 did not completely abrogate PKD activity, and hence serine 292 phosphorylation was higher than that of Gö6976. This finding suggests that phosphorylation of serine 292 in vivo is PKD- and, at least partly, PKC-dependent. In addition, we analyzed phosphorylation of serine 351 under these conditions. Surprisingly, neither PDBu stimulation nor treatment of cells with PKD and PKC inhibitors induced any detectable changes in serine 351 phosphorylation (Figure 2B).

To further characterize PKD as an upstream kinase of RIN1, we cotransfected HEK293T cells with plasmids encoding PKD1 and PKD2 WT, the constitutive active (ca) variants PKD1 S738/742E and PKD2 S706/710E, and the kinase dead (kd) variants of PKD1 K612W
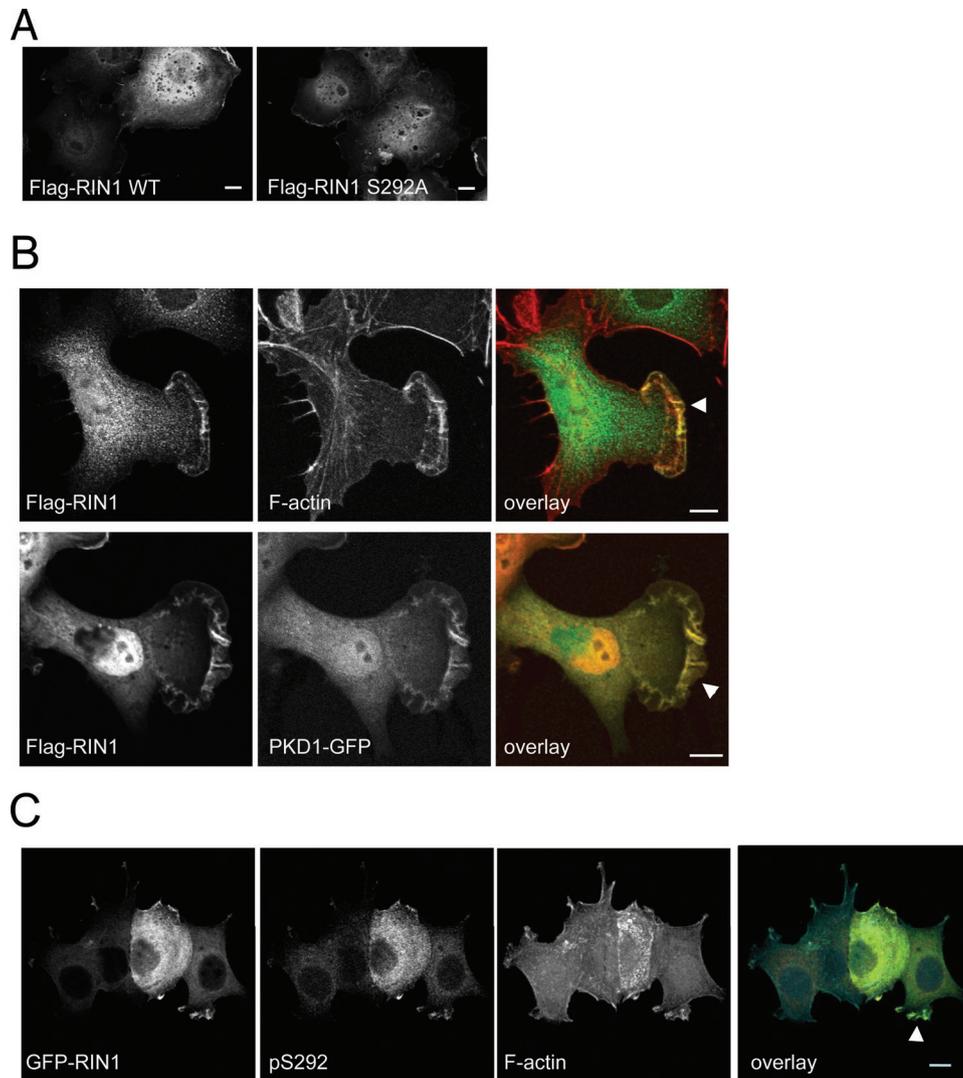
FIGURE 3: RIN1 and PKD1 colocalize at sites of actin remodeling. (A) COS7 cells were transfected with Flag-RIN1 WT and S292A expression plasmids, fixed and stained with Flag-specific antibody. The images shown are stacks of several confocal sections. Scale bar, 10 μm. (B) COS7 cells were transfected with Flag-RIN1 WT alone (top panel) or together with PKD1-GFP expression plasmid (bottom panel), fixed, and stained with Alexa546-coupled phalloidin together with Flag-specific antibody followed by Alexa488-coupled anti–mouse IgG (top panel) or Flag-specific antibody followed by Alexa546-coupled anti–mouse IgG (bottom panel). The images shown are stacks of several confocal sections. Scale bar, 10 μm. (C) MCF7 cells expressing GFP-tagged RIN1 were fixed and stained with the pS292-specific antibody followed by Alexa546-coupled anti–rabbit IgG together with Alexa633-coupled phalloidin (F-actin). The images shown are stacks of several confocal sections. Scale bar, 10 μm. Arrows indicate sites of actin remodeling.

and PKD2 K580W together with Flag-RIN1 WT. As demonstrated before, stimulation with phorbol ester increased phosphorylation at serine 292, whereas expression of PKD1kd or PKD2kd inhibited basal and stimulated serine 292 phosphorylation, proving that the PKDkd proteins act in a dominant-negative manner (Figure 2C, top panel). Interestingly, expression of PKDkd did not inhibit PDBu-induced activation of endogenous PKD proteins evident from detection with the pS910 antibody. Thus we conclude that the kd PKD proteins rather compete for substrate access than block activation of endogenous PKD. As expected, coexpression of PKD WT and PKDca proteins strongly increased basal serine 292 phosphorylation. This phosphorylation was only slightly enhanced upon PDBu stimulation. Likewise, phosphorylation of endogenous PKD proteins was increased upon coexpression of PKD WT and PKDca, suggesting that PKD proteins undergo transphosphorylation. Surprisingly, neither coexpression of active PKD variants nor PDBu stimulation induced an increase in serine 351 phosphorylation. Accordingly, expression of a kd PKD protein did not decrease phosphorylation at this site. This finding confirms that PKD is upstream of serine 292 but not of serine 351 phosphorylation. Finally, to address the question of which PKD isoform was responsible for RIN1 phosphorylation at serine 292, we used an RNA interference approach to down-regulate PKD1 and PKD2, singly and in combination in HEK293T cells, which express both PKD isoforms. Silencing of only one isoform did not influence the level of RIN1 phosphorylation as judged by immunoblotting with the pS292 antibody (Figure 2D). Simultaneous knockdown of PKD1 and PKD2, however, strongly reduced RIN1 phosphorylation, suggesting that these two isoforms were primarily responsible for phosphorylating RIN1 (Figure 2D). Of note, additional depletion of PKD3 had no effect on RIN1 phosphorylation in PKD1- and PKD2-deficient cells (unpublished data). Depletion of PKD isoforms, however, did not affect phosphorylation at serine 351. Taken together, these

results prove that RIN1 is a PKD substrate in vitro and in vivo and identify serine 292 as a novel PKD phosphorylation site in RIN1. Furthermore, our data clearly demonstrate that phosphorylation on serine 351 in vivo is independent of PKD activity in this cellular system. In the following experiments we thus focused on the functional role of serine 292 phosphorylation.

Subcellular localization of phosphorylated RIN1

RIN1 is a cytosolic protein, recruited to the plasma membrane via interaction with active Ras (Wang et al., 2002). A portion of RIN1 is also found on Rab5-positive endosomes (Tall et al., 2001). Immunofluorescence staining of Flag-tagged RIN1 in COS7 cells verified that the protein localizes mainly in the cytosol and at distinct sites of the plasma membrane. Of note, RIN1 was also located in the nucleus (Figure 3A). Next, we analyzed whether PKD-mediated phosphorylation affects the subcellular localization of the RIN1 protein (Figure 3, A and B). Neither the exchange of serine 292 to alanine in RIN1 nor the coexpression of PKD (Figure 3B) and the expression of a phosphomimetic RIN1 S292E protein, respectively, alter the localization of the protein (Figure 3A) (unpublished data).

RIN1 is a binding partner and activator of Abl tyrosine kinases, which consequently regulate actin remodeling and cell motility. Thereby, RIN1 blocks cytoskeletal rearrangements and inhibits epithelial cell migration (Hu et al., 2005). We recently demonstrated that active PKD is recruited to sites of actin remodeling at the leading edge of migrating cells upon growth factor stimulation and negatively regulates cell migration (Eiseler et al., 2007). Immunostaining of Flag-RIN1 in COS7 cells revealed that the protein colocalizes with F-actin–rich structures at the leading edge (Figure 3B, top panel, arrow). Flag-RIN1 and PKD1-GFP colocalize at these sites when coexpressed in COS7 cells (Figure 3B, bottom panel, arrow), indicating a potential interaction of the two proteins at this location. These findings were corroborated by analysis of MCF7 cells expressing GFP-tagged RIN1. Immunostaining using the pS292 specific antibody revealed that phosphorylated RIN1 colocalizes with F-actin at sites of active actin remodeling (Figure 3C, arrow).

Phosphorylation at serine 292 is critical for RIN1-mediated inhibition of cell migration

To address whether the phosphorylation at serine 292 was involved in RIN1-regulated cell migration we used Flp-In- T-Rex 293-GFP-RIN1 WT cells. Treatment of these cells with doxycycline led to a sevenfold increase in the phosphorylation of the Abl kinase substrate CrkL at tyrosine 207. The phosphorylation of CrkL was dependent on the activity of Abl tyrosine kinases as treatment of cells with STI571, a potent Abl tyrosine kinase inhibitor, completely blocked the RIN1-mediated induction of CrkL phosphorylation (Figure 4A). It has been proposed that RIN1 is an inhibitor of epithelial cell migration (Hu et al., 2005). Consequently, directed migration of cells expressing RIN1-WT was significantly decreased (p < 0.0001) compared to control cells in a Transwell assay using fetal calf serum (FCS) as chemoattractant (Figure 4B). PKD has also been described to negatively regulate epithelial cell migration. To address whether serine 292 phosphorylation modulates RIN1-regulated cell migration we induced cells to express GFP-RIN1 WT and the S292A mutant. Furthermore, we created cells expressing a phospho-mimic mutant in which serine was replaced by glutamic acid (S292E). Cells were then subjected to a chemotactic Transwell assay in the absence or presence of STI571. Mutation of serine 292 to an alanine was found to completely abrogate the RIN1 WT–induced inhibition of cell migration, whereas the S292E mutation slightly enhanced the RIN1 WT–mediated effect (Figure 4B). In addition, we demonstrated that

inhibition of cell migration by RIN1 expression is mediated via activation of Abl tyrosine kinases: The presence of STI571 completely rescued migration of cells expressing RIN1 WT and the S292E mutant, whereas no effect was observed in cells expressing RIN1-S292A (Figure 4B). Accordingly, FCS stimulation of starved cells enhanced PKD activity and CrkL phosphorylation (Figure 4C, left panel), whereas treatment of cells with the PKD inhibitor Gö6976 strongly decreased CrkL phosphorylation in control and in RIN1-expressing cells (Figure 4C, right panel), indicating that PKD-mediated phosphorylation of serine 292 modulates RIN1's ability to inhibit cell migration via activation of Abl tyrosine kinases.

To test whether phosphorylation of serine 292 affects Abl kinase activation, we made use of a genetically encoded fluorescence resonance energy transfer (FRET)-based Abl kinase biosensor, termed Abl FRET reporter (Ting et al., 2001). This sensor consists of the truncated Abl substrate CrkII, and the fluorescence donor–acceptor pair cyan fluorescent protein (CFP) and yellow fluorescent protein (YFP). On activation by Abl kinase–mediated phosphorylation of CrkII, an intramolecular complex between the tyrosine phosphorylation site and the CrkII SH2 domain is formed, modifying the orientation of the fusion protein and allowing FRET to occur. To analyze the effect of RIN1 on Abl kinase activity in vivo we transiently expressed the Abl FRET reporter alone or together with increasing amounts of Flag-tagged RIN1 WT in HEK293T cells. Coexpression of RIN1 led to an increase in the emission ratio compared to cells expressing only the Abl FRET reporter. The activation was dependent on the RIN1 concentration reaching a maximum at a 1:5 ratio and was comparable to Bcr-Abl–induced activation of the FRET reporter (Supplemental Figure 2). The RIN1-mediated activation can be attributed in part to PKD-mediated phosphorylation of the protein at serine 292 because a RIN1-S292A protein had a significantly weaker effect, whereas the RIN1-S292E protein was comparable to the WT protein at a 1:3 ratio (Figure 4D). PKD is activated downstream of Abl kinases and novel PKCs during oxidative stress signaling (Storz et al., 2003, 2004). Recent studies demonstrated that active PKD negatively regulates breast cancer cell migration (Eiseler et al., 2009; Peterburs et al., 2009). Thus it is conceivable that RIN1-mediated activation of Abl kinases in turn activates PKD and thereby inhibits cell migration. We therefore analyzed whether expression of RIN1 induces PKD activation in an Abl kinase–dependent manner. To this end we used Flp-In T-Rex-293 cells inducibly expressing GFP-tagged PKD1 and analyzed PKD1 activity in the presence or absence of RIN1 and the Abl kinase inhibitor STI571. PKD1 activation loop phosphorylation neither increased upon RIN1 expression nor decreased in response to Abl kinase inhibition compared to the control (Figure 4E). Thus PKD does not appear to be a downstream target of Abl kinases under these experimental conditions. Collectively, our data demonstrate that PKD-mediated phosphorylation regulates RIN1's ability to suppress cell migration in an Abl kinase–dependent manner.

DISCUSSION

In this study we identify a novel PKD phosphorylation site, serine 292, in RIN1. Phosphorylation at this site is specifically mediated by PKD1 and PKD2 is in accordance with previously reported overlapping substrate specificities of PKD1 and PKD2. For example, PKD1 and PKD2 were both shown to phosphorylate phosphatidylinositol 4-kinase IIIβ and ceramide transfer protein (CERT) (Hausser et al., 2005; Fugmann et al., 2007). We could show that expression of a phosphorylation-deficient RIN1 S292A variant restored epithelial cell migration compared to the WT RIN1 protein. Furthermore, PKD and phosphorylated RIN1 colocalize at sites of actin remodeling at
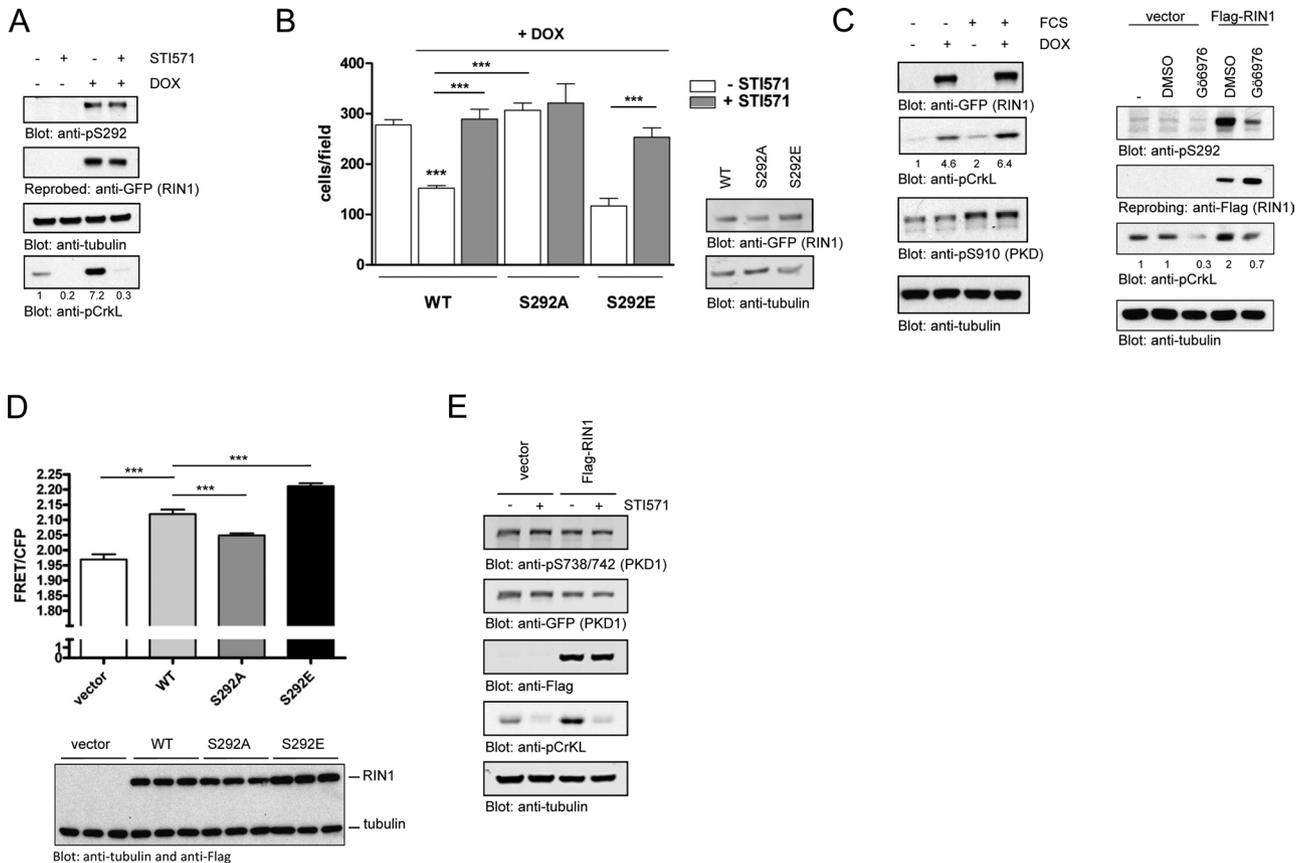
FIGURE 4: Phosphorylation of RIN1 at serine 292 coordinates cell migration in an Abl kinase–dependent manner. (A) Flp-In T-Rex-293-GFP-RIN1 WT cells were either left untreated or were treated with doxycycline (Dox) for 17 h, followed by incubation with STI571 for 1 h. Phosphorylation and expression of RIN1 were analyzed with the pS292 and a GFP-specific antibody, respectively; phosphorylation of CrkL was assessed with a pCrkL-specific antibody; and detection of tubulin verified equal protein levels. CrkL phosphorylation was quantified using ImageJ and normalized to tubulin levels. (B) Flp-In T-Rex-293-GFP-RIN1 cells were left untreated (WT) or treated with Dox (WT, S292A, S292E) for 17 h. Cells were seeded on Transwell filters, and migration was induced by an FCS gradient in the absence or presence of STI571. Expression of the RIN1 proteins was confirmed by Western blotting using a GFP-specific antibody. Detection of tubulin verified equal protein levels. Significance of differences was analyzed by an unpaired, two-tailed Student's *t* test. ***p < 0.0001. The assay is representative of three experiments performed under the same settings. (C) Left panel: Flp-In T-Rex-293-GFP-RIN1 WT cells were either left untreated or were treated with doxycycline (Dox) for 17 h. Following serum starvation overnight, cells were left untreated or stimulated with 10% serum for 10 min. Right panel: HEK293T cells were transfected with an empty vector or Flag-RIN1 expression plasmid. After 24 h, cells were treated with Gö6976 or dimethyl sulfoxide as described in Figure 2B. Expression of RIN1, phosphorylation of CrkL, and autophosphorylation of PKD were determined as described in Figure 2B. Detection of tubulin verified equal protein levels. CrkL phosphorylation was quantified using ImageJ and normalized to tubulin levels. (D) HEK293T cells were cotransfected with plasmids encoding the Abl kinase reporter and Flag-RIN1 WT, S292A, S292E, or empty vector in a 1:3 ratio. The next day, the emission ratio of the Abl kinase reporter was determined by measuring YFP (FRET) and CFP fluorescence (excitation, 433 nm) in cell lysates. Columns, mean of 12 samples; bars, SEM. Significance of differences was analyzed by an unpaired, two-tailed Student's *t* test. ***p < 0.0001. Three of 12 samples were analyzed for equal expression of RIN1 proteins. Equal protein levels were verified by tubulin detection. (E) Flp-In T-Rex-293-PKD1-GFP WT cells were treated with Dox for 24 h to induce protein expression. Cells were transfected with empty vector or Flag-RIN1 expression plasmid 24 h later and were left untreated or were treated with STI571 for 1 h. Expression of RIN1 proteins and phosphorylation of CrkL were assessed using GFP- and pCrkL-specific antibodies, respectively. Detection of tubulin served as a control.

the leading edge of migrating cells. We further demonstrate that the previously identified phosphorylation at serine 351 is not dependent on PKD in vivo. This result is in contrast with those obtained by Wang and coworkers, who demonstrated PKD-mediated phosphorylation of serine 351 using an in vitro kinase assay and metabolic labeling of COS7 cells in the presence or absence of ectopically expressed PKD (Wang *et al.*, 2002). Although we could confirm the results obtained from the in vitro kinase assay (Figure 2A), neither inhibition (Figure 2, B and D) nor activation of endogenous PKD

(Figure 2B) affected phosphorylation of serine 351 in HEK293 cells. Phosphorylation at this site induces the binding of 14–3-3 proteins, a mechanism that is common for a number of PKD substrates (Hausser *et al.*, 2006; Peterburs *et al.*, 2009; Scholz *et al.*, 2009). Notably, PKD, MAP kinase-activated protein kinase 2 (MAPKAP2), MAP/microtubule affinity-regulating kinase (MARK), and Calmodulin-dependent protein kinase II (CaMKII) show similarities in terms of active sites and substrate specificity (Doppler *et al.*, 2005; McKinsey, 2007). For example, phosphorylation of histone deacetylase 5

(HDAC5) on conserved residues induces the binding to 14–3-3 proteins and is dependent on a signaling pathway involving CaMKII and PKD in cardiac myocytes (Wu *et al.*, 2006). It is thus conceivable that, depending on cell type and stimulus, these kinases contribute to RIN1 phosphorylation at serine 351 in vivo.

At the plasma membrane, RIN1 has been demonstrated to interact with and activate Abl tyrosine kinases. RIN1 directly binds to the SH3 and SH2 domains of c-Abl and Arg, thereby stimulating kinase activity, possibly by inducing a conformational change. Subsequently, RIN1 becomes tyrosine phosphorylated by Abl kinases, a process further stabilizing the interaction of the proteins. RIN1-mediated activation of Abl kinases is followed by increased phosphorylation of the Abl kinase substrate CrkL (Hu *et al.*, 2005). Abl tyrosine kinases are important regulators of cytoskeletal rearrangements and cell migration; however, existing evidence regarding the role of Abl kinases in cell migration is conflicting. Several reports demonstrate that active Abl kinases promote cell migration and/or invasion (Srinivasan and Plattner, 2006; Stuart *et al.*, 2006. In contrast, reduced activity of Abl and Arg kinases leads to increased cell migration in immortalized cell lines. Cells lacking Abl and Arg by genetic deletion (abl –/– arg –/–) exhibit an enhanced ability to migrate in a haptotactic and chemotactic manner relative to WT cells. Conversely, overexpression of either Abl or Arg inhibited cell migration most likely by uncoupling the CrkII-CAS (Crk-associated substrate) complex (Kain and Klemke, 2001). In addition, Abl and its substrate CrkII collaborate with Rho-ROCK1 to induce cell retraction (Huang *et al.*, 2008). A recent study suggests that Arg restricts actomyosin contractility and thereby controls coupling of the cell to the substrate via focal adhesions (Peacock *et al.*, 2007). In line with the reported negative role of Abl in cell migration, overexpression of the Abl activator RIN1 negatively regulated receptor tyrosine kinase (RTK)-mediated cell migration, whereas siRNA-mediated knockdown of RIN1 led to increased migration and invasion of epithelial cells (Hu *et al.*, 2005, 2008). We show here that RIN1-mediated inhibition of epithelial cell migration is dependent on Abl kinase activation. Furthermore, we demonstrate that this process is modulated by PKD-mediated phosphorylation of serine 292. Serine 292 is located within the Abl binding domain and in close proximity to the proline-rich region, which mediates binding of RIN1 to the SH3 domain of Abl kinases (Bliss *et al.*, 2005). Mechanistically this resembles extracellular signal-regulated kinase–mediated phosphorylation of cortactin, which liberates the intramolecular interaction of cortactin's SH3 domain with the proline-rich domain. This liberation in turn allows cortactin to interact with and activate neuronal Wiskott-Aldrich Syndrome protein (N-WASP) via its liberated proline-rich regions (Martinez-Quiles *et al.*, 2004). Although RIN1 does not possess a genuine SH3 interaction domain, phosphorylation of serine 292 could facilitate or stabilize initial binding between RIN1 and Abl kinases by inducing conformational changes enabling interaction of the proline-rich region with the Abl SH3 domain. Abl and Arg have been reported to localize to sites of F-actin remodeling, such as membrane ruffles or the leading edge of migrating cells (Lewis *et al.*, 1996; Woodring *et al.*, 2002, 2003). Interestingly, our data show that phosphorylated RIN1 is present at these structures, making it likely that both proteins interact at these sites. Thus PKD-mediated RIN1 phosphorylation could be important for fine-tuning local Abl kinase activity at the leading edge of migrating cells.

Besides the activation of Abl kinases, RIN1 activates Rab5 via its GEF domain (Tall *et al.*, 2001) and promotes clathrin-mediated endocytosis of tyrosine kinase receptors, such as EGFR (Barbieri *et al.*, 2003). A study in *Drosophila melanogaster* demonstrated that the RIN1 homologue Sprint cooperates with Cbl at the front of border cells in the spatial control of receptor tyrosine kinase signaling to ensure accurate migration (Jekely *et al.*, 2005). A function for PKD in Rab4-dependent recycling of $\alpha_v\beta_3$ integrin has been demonstrated (White *et al.*, 2007). It is thus intriguing to speculate that PKD-mediated phosphorylation could be involved in the regulation of RIN1's GEF activity toward Rab5.

PKD directly interacts with F-actin and localizes to F-actin cortical structures (Eiseler *et al.*, 2007), making it likely that PKD is involved in processes regulating cytoskeletal remodeling and cell migration. Indeed, overexpression of PKD WT strongly inhibited migration of cells, whereas expression of a dominant-negative PKD variant significantly increased cell migration compared to the control (Eiseler *et al.*, 2007). Recent studies identified the cofilin phosphatase SSH1L as a physiological PKD substrate (Eiseler *et al.*, 2009; Peterburs *et al.*, 2009). PKD-mediated phosphorylation inhibits the activating interaction of SSH1L with F-actin. Consequently, the actin depolymerization factor cofilin is kept in an inactive status. Thus PKD inhibits the generation of free barbed ends at the front of motile cells, actin filament assembly, and membrane protrusion. Recent data also indicate a direct role for PKD in actin polymerization and lamellipodia extension through phosphorylation of cortactin (Eiseler *et al.*, 2010). Our data on the interplay of PKD and RIN1 suggest that PKD uses multiple modulators and substrates to regulate cell migration. It will be important to determine precisely when and where the PKD substrates SSH1L, cortactin, and RIN1 are phosphorylated and how this contributes to actin remodeling and cell migration. RIN1 has been characterized as a negative regulator of tumor cell invasive growth. Of note, a RIN1 mutant that is deficient in binding to and activating Abl kinase was unable to block cell invasion, implicating a critical role for Abl kinases in this process (Milstein *et al.*, 2007). In addition, knockdown of PKD1 by RNA interference promoted the invasiveness of cell lines that expressed PKD1 at relatively high levels (Kim *et al.*, 2008). Future studies will address whether PKD and RIN1 cooperate in invasion of breast tumor cells.

MATERIALS AND METHODS
DNA constructs, reagents, and antibodies
Full-length human RIN1 cDNA was amplified by PCR with primers containing *Eco*RI and *Xho*I restriction sites using the RZPD clone IRAUp969F0865D6 as a template and cloned into pCR3.V62-Met-Flag and pEGFP-C2 vector, respectively. The point mutants of RIN1 were generated by QuikChange site-directed PCR mutagenesis following the manufacturer's instructions (Stratagene, Amsterdam, The Netherlands).

To generate the inducible RIN1 expression plasmid pcDNA5/FRT/TO-EGFP-RIN1, the cDNA encoding GFP-RIN1 was excised from the pEGFP-C2-RIN1 plasmid with *Age*I and *Hpa*I and ligated with pcDNA5/FRT/TO digested with *Eco*RV. Integrity of all constructs was verified by sequencing. Plasmids encoding PKD1 and PKD2 WT, ca PKD1-S738/742E and PKD2-S706/710E, and kd PKD1-K612W and PKD2-K508W were described previously (Hausser *et al.*, 2005, 2006; Czondor *et al.*, 2009). The Abl FRET reporter (Ting *et al.*, 2001) was provided by Roger Tsien (University of California at San Diego). An expression plasmid encoding Bcr-Abl was obtained from Michaela Scherr (Hannover Biomedical Research School, Hannover, Germany). Antibodies specific for PKD1 autophosphorylation at serine 910 and activation loop phosphorylation at serines 738 and 742, respectively, have been described elsewhere (Hausser *et al.*, 2002). Commercially available antibodies used were as follows: anti-PKD2 rabbit

polyclonal antibody (Calbiochem, Darmstadt, Germany), anti-PKD1 C-20 rabbit polyclonal antibody (Santa Cruz Biotechnology, Heidelberg, Germany), anti–Flag M2 and anti-Abl mouse monoclonal antibody (clone ABL-148) (both Sigma-Aldrich, Munich, Germany), anti–tubulin α mouse monoclonal antibody (Neomarkers, Fremont, CA), and anti-GFP mouse monoclonal antibody (Roche Diagnostics, Mannheim, Germany). The rabbit polyclonal antibodies anti-PKD pMOTIF and phospho-CrkL (Tyr207) were obtained from Cell Signaling (Freiburg, Germany). The polyclonal anti-pS292 and anti-pS351 antibodies were generated by immunizing rabbits with the peptides NH2-CRRES(pS) VGYR-CONH2 (amino acids 288–296 in human RIN1) and NH2-LLRSM(pS)AAFC-CONH2 (amino acids 346–354 in human RIN1), respectively. Antibodies were purified from rabbit serum using immuno-affinity columns used with the phosphorylated peptides. Secondary antibodies used were Alexa488, Alexa546, or Alexa633 coupled goat anti–mouse and anti–rabbit immunoglobulin G (IgG) (Invitrogen, Darmstadt, Germany), goat anti–mouse and anti–rabbit IgG coupled to IRdye680 and IRdye800 (LI-COR Biosciences, Bad Homburg, Germany), respectively, and horseradish peroxidase (HRP) coupled goat anti–mouse and anti–rabbit IgG (Dianova, Hamburg, Germany). Alexa546- and Alexa633-coupled phalloidin was obtained from Invitrogen.

Purification of Flag-RIN1 and nanoLC/ES-MS/MS
HEK293T cells were transfected with expression plasmids for Flag-RIN1 and PKD1ΔPH-GFP. Cells were lysed 24 h after transfection, and Flag-RIN1 was immunoprecipitated with Flag-M2-Agarose (Sigma-Aldrich) according to the manufacturer's instructions. Immunoprecipitates were washed three times with lysis buffer, three times with phosphate-buffered saline (PBS), and Flag-RIN1 was eluted from the beads with 100 nM glycin, pH 2.5, and immediately neutralized using 1.5 M Tris, pH 8.8. Eluted protein was separated on a NuPAGE 4–12% Bis-Tris Gel (Invitrogen) and stained with colloidal Coomassie. The SDS–PAGE–separated Flag-RIN1 fusion protein was tryptically digested in gel as previously described (Shevchenko et al., 1996). The extracted peptides were analyzed by nanoLC/ES-MS/MS using an HCTplus ion trap mass spectrometer (Bruker-Daltonics, Bremen, Germany) (Tolson et al., 2006). High-performance liquid chromatography was performed on a 150 mm × 75 μm (ID) Vydac Everest C18 (5 μm, 300 Å) capillary column (Alltech Grom, Rottenburg-Hailfingen, Germany). Peptides were eluted (250 nl/min flow rate) in the gradient mode: 0–3 min 5–8% B, 3–93 min 8–40% B, 93–123 min 40–95% B, where system A was 0.1% formic acid in water (vol/vol) and system B was 0.1% formic acid and 80% acetonitrile in water (vol/vol). The data-dependent MS/MS analyses included the acquisition of a survey spectrum (m/z 300–1,500) followed by MS/MS spectra (m/z 100–2,500) of the four most abundant ions in the survey scan. Uninterpreted MS/MS data were searched using MASCOT (www.matrixscience.com). Assignments of the phosphopeptides were confirmed by manual comparison of the MS/MS mass spectra with the predicted fragmentations generated by the MS-Product component of ProteinProspector (http://prospector.ucsf.edu/).

Cell culture
HEK293T, MCF7, and COS7 cells were maintained in RPMI 1640 medium supplemented with 10% FCS. For transient transfections, HEK293T cells were transfected with TransIT293 (Mirus Bio Corporation, Madison, WI) according to the manufacturer's instructions. In the case of siRNA oligonucleotides, HEK293T cells were transfected with Oligofectamine (Invitrogen) according to the

manufacturer's instructions. After 48 h, cells were transfected with pCR3.V62-Met-Flag-RIN1 and harvested 24 h later. siRNA oligonucleotides used were 5′-gucgagagaagaggucaaatt-3′ (PKD1) and 5′-gcaaagacugcaaguuuaatt-3′ (PKD2). As a control, a lacZ-specific siRNA was used (5′-gcggcugccggaauuuacctt-3′). All oligonucleotides were purchased from MWG Biotech, Ebersberg, Germany. COS7 and MCF7 cells were transfected with Lipofectamine 2000 (Invitrogen). Treatment of cells with Gö6976 or Gö6983 (Calbiochem) was at 5 μM for 1 h prior to stimulation. Treatment of cells with PDBu (Sigma-Aldrich) was at 1 μM for 15 min. STI571 (gift from Heiko von der Kuip, Robert-Bosch Hospital, Stuttgart, Germany) was used at 10 μM.

Flp-In T-Rex-293 cells (Invitrogen) were grown in DMEM containing 10% FCS, zeocin at 100 μg/ml, and blasticidin at 15 μg/ml. These cells stably express the Tet repressor and contain a single FRT site and were used to generate the Flp-In-RIN1 lines. Cells were cotransfected with pcDNA5/FRT/TO-EGFP-RIN1 WT, S292A, and S292E, respectively, and the Flp recombinase expression plasmid pOG44 at a ratio of 1:10 and then selected with hygromycin at 100 μg/ml. Induction of protein expression with doxycycline was at 10 ng/ml.

Immunofluorescence and microscopy
Transfected COS7 and MCF7 cells were grown on collagen-coated coverslips, washed with PBS, fixed in 4% paraformaldehyde (PFA) at room temperature for 15 min, washed, permeabilized with 0.1% Triton X-100 (5 min, room temperature), and blocked with blocking buffer (5% FCS and 0.05% Tween 20 in PBS) for 30 min. The cells were incubated with the primary antibodies diluted in blocking buffer (1 μg/ml) for 2 h, washed, incubated with secondary antibodies diluted in blocking buffer for 1 h, washed, mounted in Fluoromount G (Southern Biotechnology, Birmingham, AL), and analyzed on a confocal laser scanning microscope (TCS SP2; Leica, Wetzlar, Germany). Alexa488 and GFP were excited with the 488-nm line of the argon laser, and fluorescence was detected at 500–535 nm. Alexa546 was excited with the 543-nm line of a helium–neon laser, and fluorescence was detected at 555–700 nm. Cells were imaged with a 40.0×/1.25 HCX PL APO objective lens. Images were processed with Adobe Photoshop.

Protein extraction of cells
Whole cell extracts were obtained by solubilizing cells in lysis buffer (20 mM Tris pH 7.4, 150 mM NaCl, 1% Triton X-100 or Nonidet P-40, 1 mM EDTA, 1 mM ethylene glycol tetraacetic acid (EGTA), plus Complete protease inhibitors and PhosSTOP [Roche Diagnostics]). Lysates were clarified by centrifugation at 16,000 × g for 15 min.

Immunoprecipitation and Western blotting
For immunoprecipitation, equal amounts of proteins were incubated with specific antibodies for 1.5 h at 4°C. Immune complexes were collected with protein G-Agarose (KPL, Gaithersburg, MD) and washed three times with lysis buffer. Precipitated proteins were released by boiling in sample buffer and were subjected to SDS–PAGE. The proteins were blotted onto nitrocellulose membranes (Pall, Dreieich, Germany). After blocking with 0.5% blocking reagent (Roche Diagnostics), filters were probed with specific antibodies. Proteins were visualized with HRP-coupled secondary antibodies using the enhanced chemiluminescence (ECL) detection system or IRdye-coupled secondary antibodies followed by analysis with Odyssey software (LI-COR Biosciences).

Kinase assay

After immunoprecipitation (with anti-Flag antibodies for transfected RIN1), the PKD kinase reaction was carried out for 15 min at 37°C in 30 μl of kinase buffer (50 mM Tris pH 7.4, 10 mM MgCl$_2$, and 2 mM dithiothreitol). Reaction was started by addition of 10 μl of a kinase buffer mixture containing 2 μCi [γ-P^{32}]-ATP and 100 ng of purified PKD1 (Dieterich et al., 1996). To terminate reaction, 10 μl of 5× SDS sample buffer was added, and the samples were resolved by SDS–PAGE, blotted onto nitrocellulose, and analyzed on a PhosphoImager Storm860 (GE Healthcare, Freiburg, Germany).

Transwell filter assay

Cell migration assays were performed using 24-well Transwell filter inserts (Corning, Corning, NY) with 8-μM pore diameter and coated at the bottom with rat collagen R type I (SERVA, Heidelberg, Germany). Flp-In T-Rex 293 cells were seeded at a density of 50,000 cells/insert, and migration was induced by an FCS gradient of 0–10% for 4 h. Migrated cells were fixed using 4% PFA, and the inside of the Transwell insert was wiped with a cotton swab to remove nonmigrated cells. To quantify migration, cells on the filter were stained with crystal violet. After washing, filters were photographed using a widefield fluorescence microscope (Leica) equipped with a CCD camera. Results were calculated as median number of migrated cells per visual field with at least four images per filter.

Abl reporter assays

HEK293T cells transiently expressing the Abl reporter and Flag-RIN1 constructs were lysed in 50 mM Tris, pH 7.5, 5 mM β-glycerophosphate, 5 mM sodium fluoride, and 0.5 Triton X-100, and debris was removed by centrifugation at $16,000 \times g$ for 10 min. Emission ratios (FRET/CFP) were determined by measuring CFP and YFP fluorescence after background subtraction at 475 and 530 nm, respectively, using a Tecan Infinite 200M plate reader (excitation, 433 nm). Expression of the RIN1 proteins was controlled by Western blot analysis using a Flag-specific antibody.

REFERENCES

Afar DE, Han L, McLaughlin J, Wong S, Dhaka A, Parmar K, Rosenberg N, Witte ON, Colicelli J (1997). Regulation of the oncogenic activity of BCR-ABL by a tightly bound substrate protein RIN1. Immunity 6, 773–782.

Barbieri MA, Fernandez-Pol S, Hunker C, Horazdovsky BH, Stahl PD (2004). Role of rab5 in EGF receptor-mediated signal transduction. Eur J Cell Biol 83, 305–314.

Barbieri MA, Kong C, Chen PI, Horazdovsky BF, Stahl PD (2003). The SRC homology 2 domain of Rin1 mediates its binding to the epidermal growth factor receptor and regulates receptor endocytosis. J Biol Chem 278, 32027–32036.

Beausoleil SA, Villen J, Gerber SA, Rush J, Gygi SP (2006). A probability-based approach for high-throughput protein phosphorylation analysis and site localization. Nat Biotechnol 24, 1285–1292.

Bliss JM, Venkatesh B, Colicelli J (2005). The RIN family of Ras effectors. Methods Enzymol 407, 335–344.

Cao X, Tanis KQ, Koleske AJ, Colicelli J (2008). Enhancement of ABL kinase catalytic efficiency by a direct binding regulator is independent of other regulatory mechanisms. J Biol Chem 283, 31401–31407.

Czondor K, Ellwanger K, Fuchs YF, Lutz S, Gulyas M, Mansuy IM, Hausser A, Pfizenmaier K, Schlett K (2009). Protein kinase D controls the integrity of Golgi apparatus and the maintenance of dendritic arborization in hippocampal neurons. Mol Biol Cell 20, 2108–2120.

Deininger K, Eder M, Kramer ER, Zieglgansberger W, Dodt HU, Dornmair K, Colicelli J, Klein R (2008). The Rab5 guanylate exchange factor Rin1 regulates endocytosis of the EphA4 receptor in mature excitatory neurons. Proc Natl Acad Sci USA 105, 12539–12544.

Dhaka A, Costa RM, Hu H, Irvin DK, Patel A, Kornblum HI, Silva AJ, O'Dell TJ, Colicelli J (2003). The RAS effector RIN1 modulates the formation of aversive memories. J Neurosci 23, 748–757.

Dieterich S, Herget T, Link G, Bottinger H, Pfizenmaier K, Johannes FJ (1996). In vitro activation and substrates of recombinant, baculovirus expressed human protein kinase C mu. FEBS Lett 381, 183–187.

Doppler H, Storz P, Li J, Comb MJ, Toker A (2005). A phosphorylation state-specific antibody recognizes Hsp27, a novel substrate of protein kinase D. J Biol Chem 280, 15013–15019.

Eiseler T, Doppler H, Yan IK, Kitatani K, Mizuno K, Storz P (2009). Protein kinase D1 regulates cofilin-mediated F-actin reorganization and cell motility through slingshot. Nat Cell Biol 11, 545–556.

Eiseler T, Hausser A, De Kimpe L, Van Lint J, Pfizenmaier K (2010). PKD controls actin polymerization and cell motility through phosphorylation of cortactin. J Biol Chem 285, 18672–18683.

Eiseler T, Schmid MA, Topbas F, Pfizenmaier K, Hausser A (2007). PKD is recruited to sites of actin remodelling at the leading edge and negatively regulates cell migration. FEBS Lett 581, 4279–4287.

Fugmann T, Hausser A, Schoffler P, Schmid S, Pfizenmaier K, Olayioye MA (2007). Regulation of secretory transport by protein kinase D-mediated phosphorylation of the ceramide transfer protein. J Cell Biol 178, 15–22.

Han L, Colicelli J (1995). A human protein selected for interference with Ras function interacts directly with Ras and competes with Raf1. Mol Cell Biol 15, 1318–1323.

Han L, Wong D, Dhaka A, Afar D, White M, Xie W, Herschman H, Witte O, Colicelli J (1997). Protein binding and signaling properties of RIN1 suggest a unique effector function. Proc Natl Acad Sci USA 94, 4954–4959.

Hausser A, Link G, Bamberg L, Burzlaff A, Lutz S, Pfizenmaier K, Johannes FJ (2002). Structural requirements for localization and activation of protein kinase C mu (PKC mu) at the Golgi compartment. J Cell Biol 156, 65–74.

Hausser A, Link G, Hoene M, Russo C, Selchow O, Pfizenmaier K (2006). Phospho-specific binding of 14–3-3 proteins to phosphatidylinositol 4-kinase III beta protects from dephosphorylation and stabilizes lipid kinase activity. J Cell Sci 119, 3613–3621.

Hausser A, Storz P, Martens S, Link G, Toker A, Pfizenmaier K (2005). Protein kinase D regulates vesicular transport by phosphorylating and activating phosphatidylinositol-4 kinase III β at the Golgi complex. Nat Cell Biol 7, 880–886.

Hu H, Bliss JM, Wang Y, Colicelli J (2005). RIN1 is an ABL tyrosine kinase activator and a regulator of epithelial-cell adhesion and migration. Curr Biol 15, 815–823.

Hu H, Milstein M, Bliss JM, Thai M, Malhotra G, Huynh LC, Colicelli J (2008). Integration of transforming growth factor beta and RAS signaling silences a RAB5 guanine nucleotide exchange factor and enhances growth factor-directed cell migration. Mol Cell Biol 28, 1573–1583.

Huang X, Wu D, Jin H, Stupack D, Wang JY (2008). Induction of cell retraction by the combined actions of Abl-CrkII and Rho-ROCK1 signaling. J Cell Biol 183, 711–723.

Jaggi M, Rao PS, Smith DJ, Wheelock MJ, Johnson KR, Hemstreet GP, Balaji KC (2005). E-cadherin phosphorylation by protein kinase D1/protein kinase Cμ is associated with altered cellular aggregation and motility in prostate cancer. Cancer Res 65, 483–492.

Jekely G, Sung HH, Luque CM, Rorth P (2005). Regulators of endocytosis maintain localized receptor tyrosine kinase signaling in guided migration. Dev Cell 9, 197–207.

Kain KH, Klemke RL (2001). Inhibition of cell migration by Abl family tyrosine kinases through uncoupling of Crk-CAS complexes. J Biol Chem 276, 16185–16192.

Kim M et al. (2008). Epigenetic inactivation of protein kinase D1 in gastric cancer and its role in gastric cancer cell migration and invasion. Carcinogenesis 29, 629–637.

Kong C, Su X, Chen PI, Stahl PD (2007). RIN1 interacts with signal transducing adaptor molecule (STAM) and mediates epidermal growth factor receptor trafficking and degradation. J Biol Chem 282, 15294–15301.

Lewis JM, Baskaran R, Taagepera S, Schwartz MA, Wang JY (1996). Integrin regulation of c-Abl tyrosine kinase activity and cytoplasmic-nuclear transport. Proc Natl Acad Sci USA 93, 15174–15179.

Martinez-Quiles N, Ho HYH, Kirschner MW, Ramesh N, Geha RS (2004). Erk/Src phosphorylation of cortactin acts as a switch on-switch off mechanism that controls its ability to activate N-WASP. Mol Cell Biol 24, 5269–5280.

McKinsey TA (2007). Derepression of pathological cardiac genes by members of the CaM kinase superfamily. Cardiovasc Res 73, 667–677.

Milstein M, Mooser CK, Hu H, Fejzo M, Slamon D, Goodglick L, Dry S, Colicelli J (2007). RIN1 is a breast tumor suppressor gene. Cancer Res 67, 11510–11516.

Peacock JG, Miller AL, Bradley WD, Rodriguez OC, Webb DJ, Koleske AJ (2007). The Abl-related gene tyrosine kinase acts through p190RhoGAP to inhibit actomyosin contractility and regulate focal adhesion dynamics upon adhesion to fibronectin. Mol Biol Cell 18, 3860–3872.

Peterburs P, Heering J, Link G, Pfizenmaier K, Olayioye MA, Hausser A (2009). Protein kinase D regulates cell migration by direct phosphorylation of the cofilin phosphatase slingshot 1 like. Cancer Res 69, 5634–5638.

Scholz RP, Regner J, Theil A, Erlmann P, Holeiter G, Jahne R, Schmid S, Hausser A, Olayioye MA (2009). DLC1 interacts with 14–3-3 proteins to inhibit RhoGAP activity and block nucleocytoplasmic shuttling. J Cell Sci 122, 92–102.

Shevchenko A, Wilm M, Vorm O, Mann M (1996). Mass spectrometric sequencing of proteins silver-stained polyacrylamide gels. Anal Chem 68, 850–858.

Srinivasan D, Plattner R (2006). Activation of Abl tyrosine kinases promotes invasion of aggressive breast cancer cells. Cancer Res 66, 5648–5655.

Storz P, Doppler H, Johannes FJ, Toker A (2003). Tyrosine phosphorylation of protein kinase D in the pleckstrin homology domain leads to activation. J Biol Chem 278, 17969–17976.

Storz P, Doppler H, Toker A (2004). Protein kinase Cdelta selectively regulates protein kinase D-dependent activation of NF-kappaB in oxidative stress signaling. Mol Cell Biol 24, 2614–2626.

Stuart JR, Gonzalez FH, Kawai H, Yuan ZM (2006). c-Abl interacts with the WAVE2 signaling complex to induce membrane ruffling and cell spreading. J Biol Chem 281, 31290–31297.

Tall GG, Barbieri MA, Stahl PD, Horazdovsky BF (2001). Ras-activated endocytosis is mediated by the Rab5 guanine nucleotide exchange activity of RIN1. Dev Cell 1, 73–82.

Ting AY, Kain KH, Klemke RL, Tsien RY (2001). Genetically encoded fluorescent reporters of protein tyrosine kinase activities in living cells. Proc Natl Acad Sci USA 98, 15003–15008.

Tolson JP, Flad T, Gnau V, Dihazi H, Hennenlotter J, Beck A, Mueller GA, Kuczyk M, Mueller CA (2006). Differential detection of S100A8 in transitional cell carcinoma of the bladder by pair wise tissue proteomic and immunohistochemical analysis. Proteomics 6, 697–708.

Wang QJ (2006). PKD at the crossroads of DAG and PKC signaling. Trends Pharmacol Sci 27, 317–323.

Wang Y, Colicelli J (2001). RAS interaction with effector target RIN1. Methods Enzymol 332, 139–151.

Wang Y, Waldron RT, Dhaka A, Patel A, Riley MM, Rozengurt E, Colicelli J (2002). The RAS effector RIN1 directly competes with RAF and is regulated by 14–3-3 proteins. Mol Cell Biol 22, 916–926.

White DP, Caswell PT, Norman JC (2007). alpha v beta3 and alpha5beta1 integrin recycling pathways dictate downstream Rho kinase signaling to regulate persistent cell migration. J Cell Biol 177, 515–525.

Woodring PJ, Hunter T, Wang JY (2003). Regulation of F-actin-dependent processes by the Abl family of tyrosine kinases. J Cell Sci 116, 2613–2626.

Woodring PJ, Litwack ED, O'Leary DD, Lucero GR, Wang JY, Hunter T (2002). Modulation of the F-actin cytoskeleton by c-Abl tyrosine kinase in cell spreading and neurite extension. J Cell Biol 156, 879–892.

Wu X, Zhang T, Bossuyt J, Li X, McKinsey TA, Dedman JR, Olson EN, Chen J, Brown JH, Bers DM (2006). Local InsP3-dependent perinuclear Ca2+ signaling in cardiac myocyte excitation-transcription coupling. J Clin Invest 116, 675–682.

Zhang Y, Wolf-Yadlin A, Ross PL, Pappin DJ, Rush J, Lauffenburger DA, White FM (2005). Time-resolved mass spectrometry of tyrosine phosphorylation sites in the epidermal growth factor receptor signaling network reveals dynamic modules. Mol Cell Proteomics 4, 1240–1250.